SUPPORTING INFORMATION

Understanding Selectivity of Metabolic Labelling and Click-Targeting in Multicellular Environments as a Route to Tissue Selective Drug Delivery

Angel Tan,*[abc] Qingtao Liu,[a] Dedy Septiadi,[c] Shuiling Chu,[c] Tianqing Liu,[d] Sarah-Jane Richards,[e] Barbara Rothen-Rutishauser,[c] Alke Petri-Fink,[c] Matthew I. Gibson,[ef] and Ben J. Boyd*[ab]

[a]Drug Delivery, Disposition and Dynamics, Monash Institute of Pharmaceutical Sciences, Monash University, Parkville Campus, VIC 3052, Australia. *Emails: angel.tan@monash.edu; ben.boyd@monash.edu

[b]ARC Centre of Excellence in Convergent Bio-Nano Science and Technology, Monash University, Parkville, VIC 3052, Australia

[c]Adolphe Merkle Institute, University of Fribourg, Chemin des Verdiers 4, 1700 Fribourg, Switzerland.

[d]NICM Health Research Institute, Western Sydney University, Westmead, NSW 2145, Australia.

[e]Department of Chemistry, University of Warwick, Gibbet Hill Road, Coventry, CV47AL, UK.

[f]Warwick Medical School, University of Warwick, Coventry, CV4 7AL, UK.

SUPPLEMENTARY RESULTS

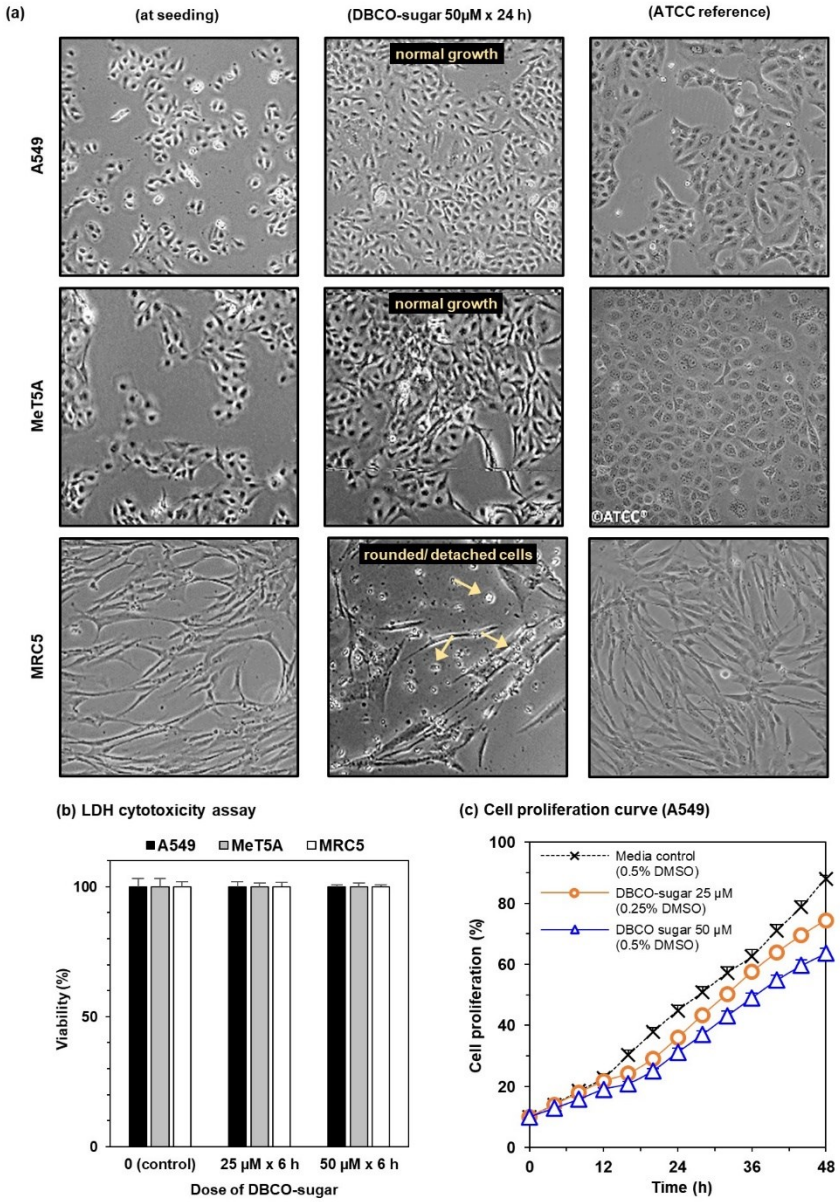

Fig. S1 Cytotoxicity screening of *N*-DBCO, tetra-*O*-acetylated, D-mannosamine (Ac_4ManNDBCO), on cancer (A549 alveolar epithelial cells) and non-cancerous (MeT5A mesothelial cells and MRC5 fibroblasts) human lung cells: **(a)** bright-field microscopy images of cells at seeding and after feeding with the DBCO-sugar at 'high dose' (50 μM) for 24 h, where A549 and MeT5A cells showed normal growth and appearance, whereas MRC5 cells presented unhealthy, rounded appearance and detachment from the culture dish; **(b)** viability of cells based on lactate dehydrogenase (LDH) cytotoxicity assay, where all three cell lines fed with Ac_4ManNBCO at a 'low' (25 μM) and a 'high' (50 μM) dose, respectively for 6 h did not elicit significant LDH release (which is representative of cellular membrane damage) relative to the negative controls (mean ± S.D., n = 3); **(c)** IncuCyte® cell proliferation assay of A549 cells at 0–50 μM of Ac_4ManNDBCO showing significant retardation in the cell growth particularly post-12 h (mean ± S.E., n = 12).

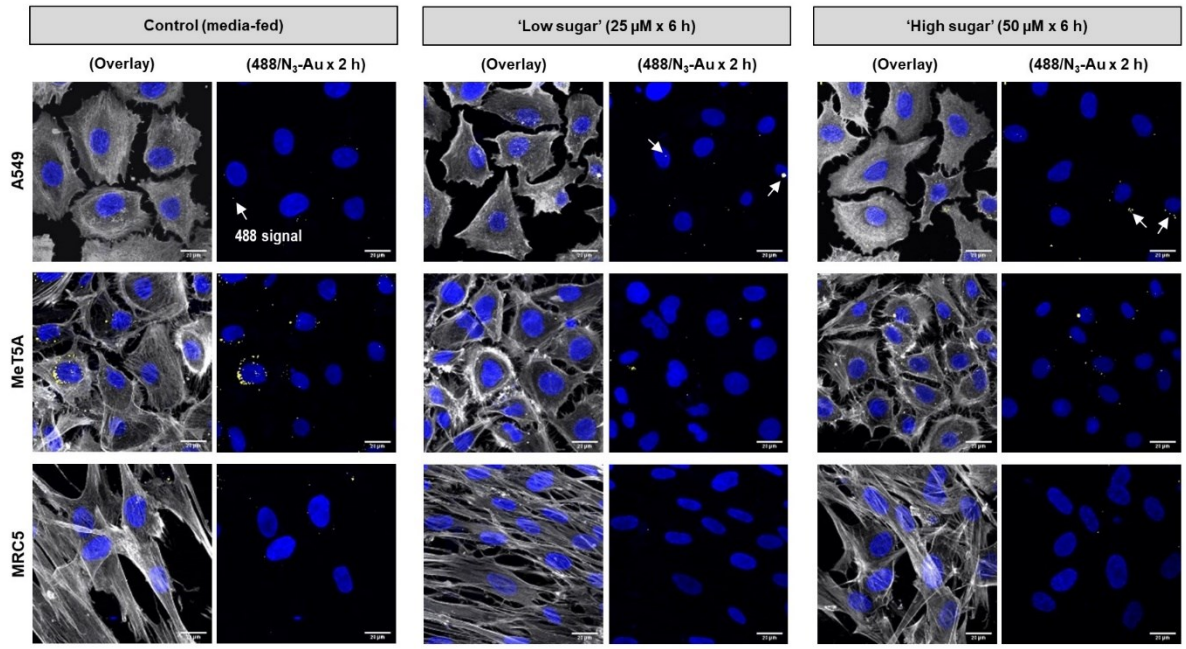

Fig. S2 Comparative binding/ uptake of 488/N_3-AuNps in A549/MeT5A/MRC5 multicellular culture: CLSM images of media-fed control cells and DBCO-sugar treated cells at a 'low dose' (25 µM) and 'high dose' (50 µM) for 6 h, followed by co-exposure to 488/N_3-AuNps (at 100 µM in Au concentration for 2 h) at 37 °C, 5% CO_2. The cell nuclei were stained with DAPI (blue), the F-actin filaments with rhodamine phalloidin (grey) and the N_3-AuNps indicated by the 488 fluorescence signals (yellow). Scale bar = 20 µm.

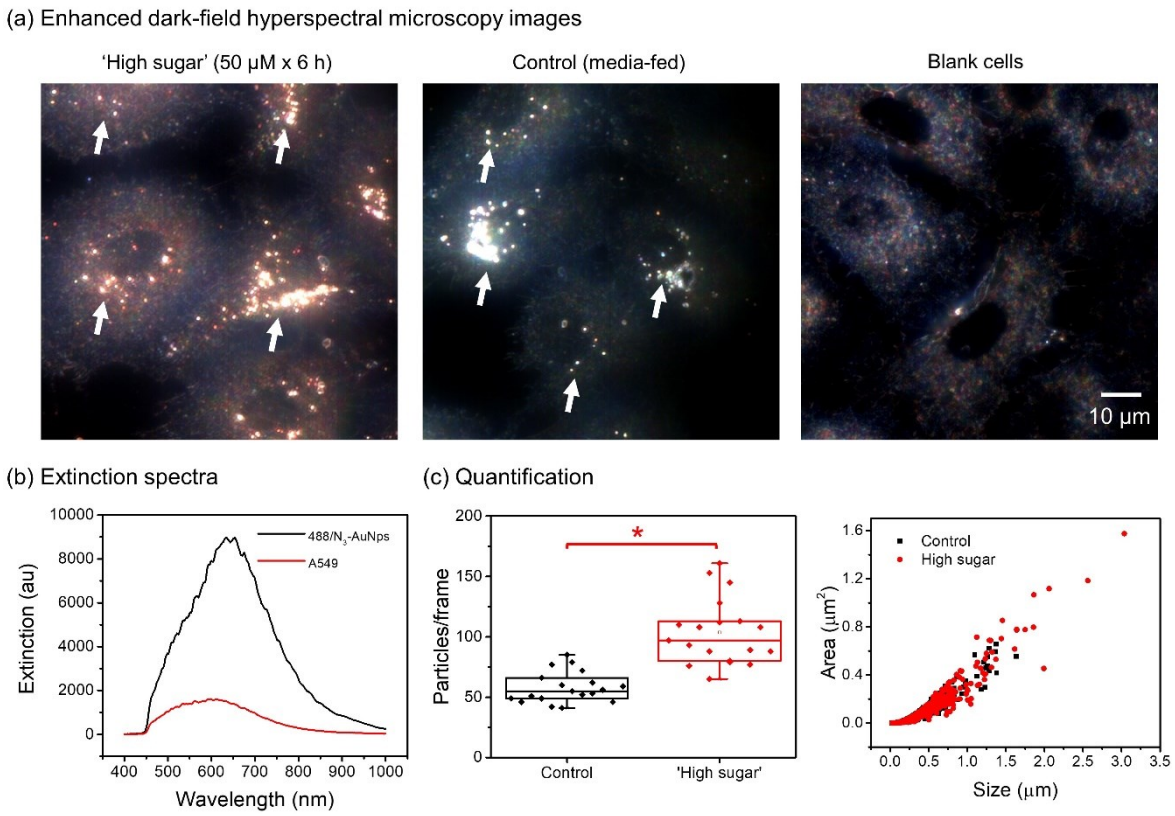

Fig. S3 Enhanced dark-field hyperspectral optical microscopy of 488/N_3-AuNps in A549 cells: **(a)** microscopy images of cells treated with DBCO-sugar at 'high dose' (50 µM) for 6 h and media-fed control cells, followed by exposure to 488/N_3-AuNps (at 100 µM in Au concentration for 20 h) at 37 °C, 5% CO_2. The bright, yellowish spots correspond to the 488/N_3-AuNps (as indicated by the white arrows); **(b)** extinction spectra of AuNps and blank cells showing strong detection signals for Au; and **(c)** quantitative image analysis based on particle number or aggregate per image frame (mean ± error, $n = 19$, $*p < 0.05$ using one-way ANOVA test), and distribution of size and area of each individual particles showing formation of small and large agglomerates.

EXPERIMENTAL DATA

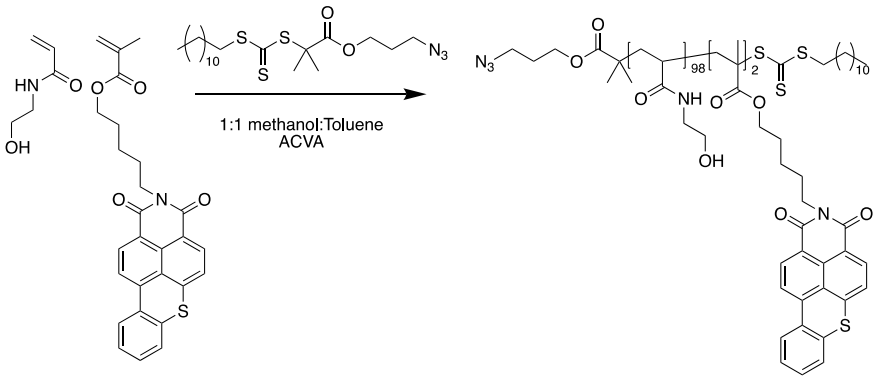

Scheme S1 Synthetic procedure for the RAFT copolymerisation of *N*-hydroxyethyl acrylamide (HEA) and hostasol methacrylate.

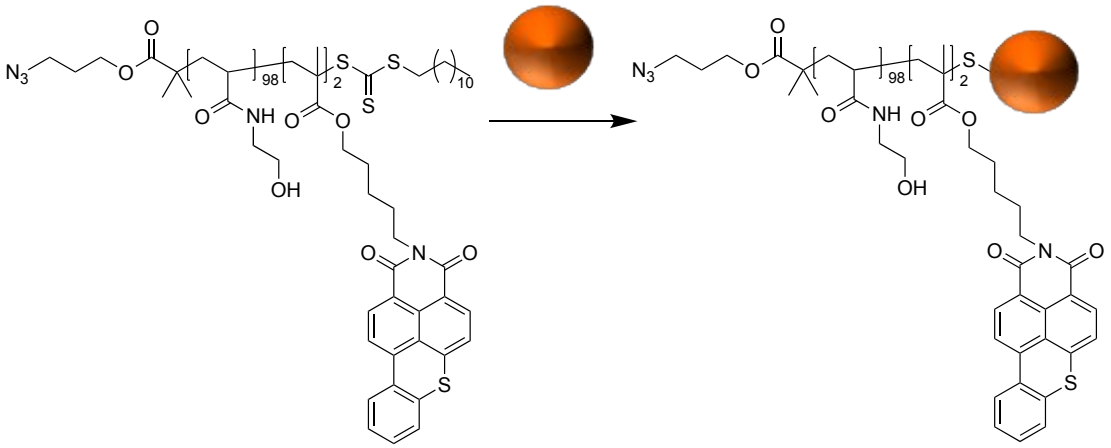

Scheme S2 Functionalisation of AuNps with p(HEA_{98}-co-HMA_2) (488/N_3-AuNps).

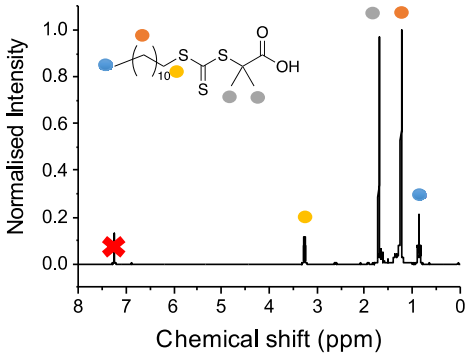

Fig. S4 ^{1}H NMR of 2-(dodecylthiocarbonothioylthio)-2-methylpropionic acid (DMP).

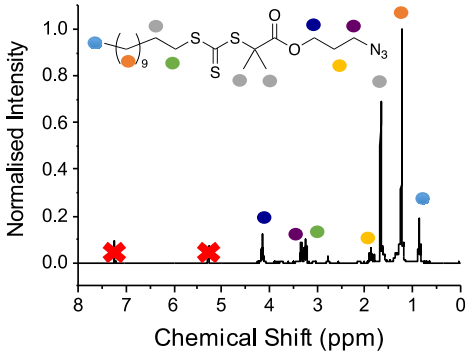

Fig. S5 ^{1}H NMR of 2-(dodecylthiocarbonothioylthio)-2-methylpropionic acid 3-azido-1-propanol ester (N_3-DMP).

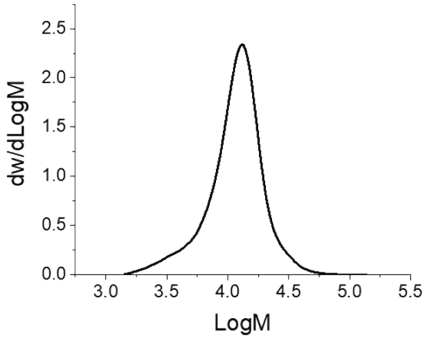

Fig. S6 SEC of poly(*N*-hydroxyethyl acrylamide-co-hostasol methacrylate).

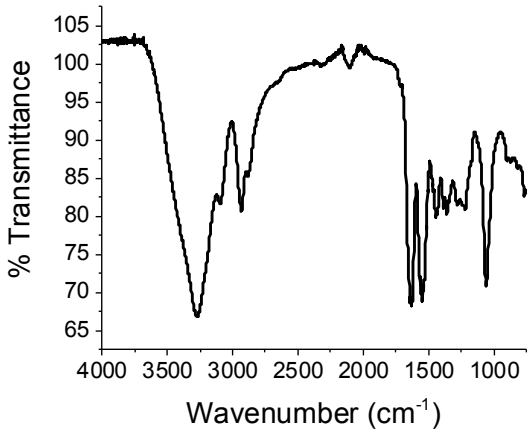

Fig. S7 IR of poly(*N*-hydroxyethyl acrylamide-co-hostasol methacrylate).

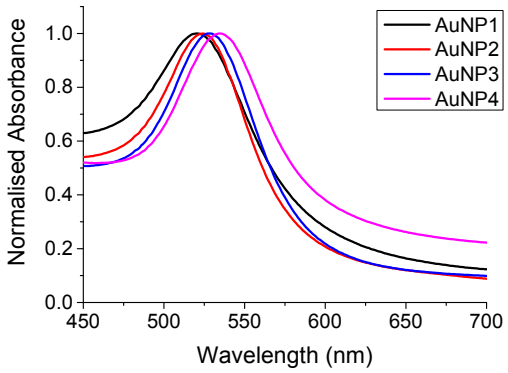

Fig. S8 UV-visible spectrum of the gold nanoparticles (AuNps), where the batch of 30 nm (AuNp2, red) was used in this study.

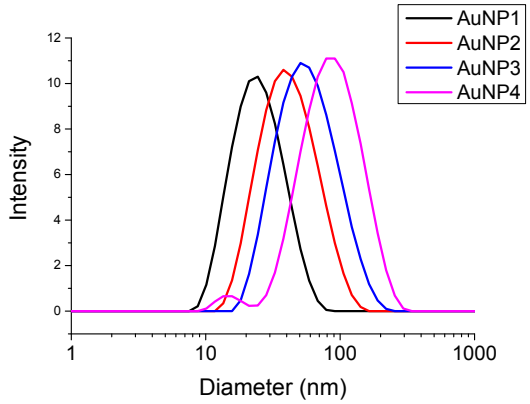

Fig. S9 Size distributions of AuNps from dynamic light scattering: black 15 nm, red 30 nm, blue 45 nm, pink 60 nm. The batch of 30 nm (AuNp2, red) was used in this study.

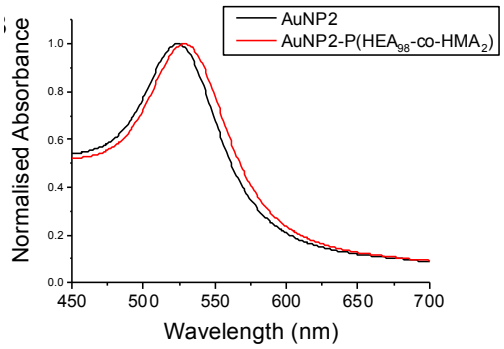

Fig. S10 UV-vis spectra of gold nanoparticles (core diameter = 30 nm) before (black line, AuNps) and after (red line, 488/N_3-AuNps) functionalisation with p(HEA_{98}-co-HMA_2).

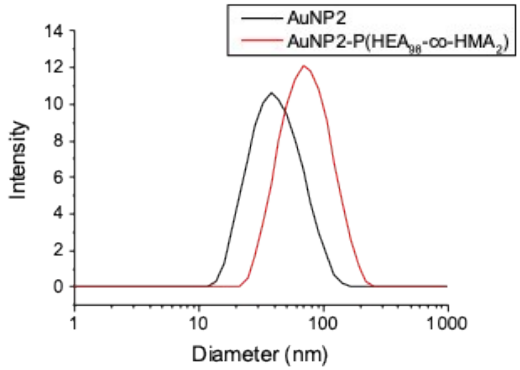

Fig. S11: Size distribution of gold nanoparticles (core diameter = 30 nm) from dynamic light scattering: before (black line, AuNps) and after (red line, 488/N_3-AuNps) functionalisation with p(HEA_{98}-co-HMA_2).

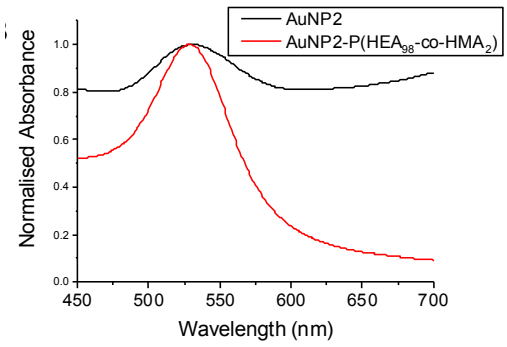

Fig. S12: UV-vis spectra of gold nanoparticles (core diameter = 30 nm) after incubation in PBS before (black line, AuNps) and after (red line, 488/N_3-AuNps) functionalisation with p(HEA_{98}-co-HMA_2).

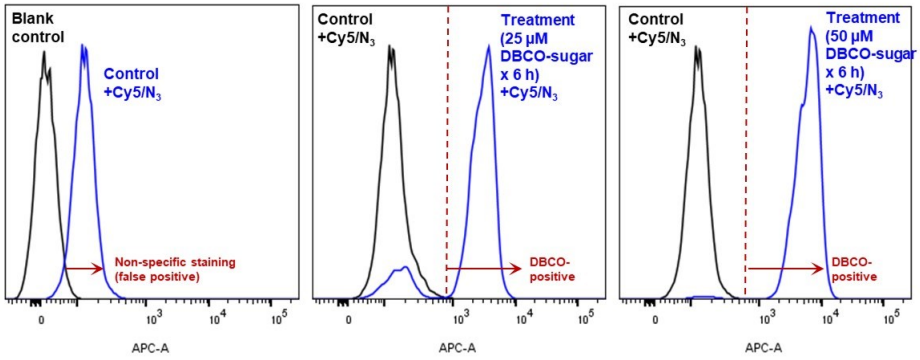

Fig. S13 Representative histograms from flow cytometric analysis showing the peak shifts towards the right along the x-axis indicating higher Cy5 fluorescence intensity in the presence of non-specific $Cy5/N_3$ binding (*i.e.*, Control+$Cy5/N_3$ > Blank control) and specific DBCO-N_3 reactions in the DBCO-sugar treated populations.

Particle	λ_{SPR} (nm)	A_{SPR}/A_{450}	Diameter (nm)	
			UV-vis	DLS
$AuNP_1$	520	1.59	14	24
$AuNP_2$	**524**	**1.85**	**30**	**32**
$AuNP_3$	528	1.97	42	48
$AuNP_4$	534	1.90	56	62

Table S1 Summary of the UV-vis and DLS determined diameter of the particles.

Table S2 Summary of the UV-vis and DLS derived diameters of the p(HEA_{98}-co-HMA_2)-functionalised gold nanoparticles (488/N_3-AuNps).

Particle	λ_{SPR} (nm)	A_{SPR}/A_{450}	Diameter (nm)	
			UV-vis	DLS
488/N_3-$AuNps_{15}$	525	1.61	32	--
488/N_3-$AuNps_{30}$	**529**	**1.83**	**44**	**50**
488/N_3-$AuNps_{45}$	532	1.96	42	70
488/N_3-$AuNps_{60}$	539	1.95	66	110

Table S3 Supplemented cell culture media for A549 adenocarcinomic alveolar basal epithelial cells, MeT5A mesothelial cells, and MRC5 fibroblasts.

Cell line	Culture medium	Subculture ratio
A549	Roswell Park Memorial Institute (RPMI-1640) medium supplemented with fetal bovine serum (FBS, 10%), L-glutamine (1%), penicillin/streptomycin (1%) (all Gibco, MD USA)	1:10
MeT5A	Medium 199 containing FBS (10%, Gibco, MD USA), epidermal growth factor (3.3 nM), hydrocortisone (400 nM), zinc-free bovine insulin (870 nM), HEPES (20 mM, Gibco, USA), penicillin/streptomycin (1%) (all Sigma-Aldrich, MO USA)	1:5
MRC5	Dulbecco's Modified Eagle Medium (DMEM) containing FBS (10%), L-glutamine (1%), non-essential amino acids (1%), penicillin/streptomycin (1%) (all Gibco, MD USA)	1:4